A Ray-Tracing Based Fingerprinting for Indoor Positioning

Tsai-Mau Wang, Po-Hsuan Tseng, Yao-Chia Chan, Ding-Bing Lin
Department of Electronic Engineering
National Taipei University of Technology, Taipei, Taiwan
{t101418104, phtseng, dblin}@ntut.edu.tw, yaochia.chan@gmail.com

***Abstract*—Indoor wireless positioning technique has huge market value and is one of the most active research topics in recent years. Received signal strength (RSS) measurement is the main category in wireless positioning technique since the information of RSS can be collected easily. With the rapidly development of OFDM-based wireless broadband system, channel impulse response (CIR) measurement and more accurate RSS measurement can be obtained. In the paper, we develop a OFDM-based channel sounding system to perform a series of channel measurement experiments to collect offline and online measurements. Moreover, the ray-tracing (RT) technique is utilized to simulate CIR measurement. We propose a ray-tracing based fingerprinting (RBFP) positioning technique, which evaluates the similarity between the online measurement and the simulated CIR database using RT. The error of the proposed RBFP is validated in the experiment that has performance comparable with the traditional fingerprinting (FP).**

***Index Terms*—received signal strength, channel impulse response, channel frequency response, indoor location estimation**

I. Introduction

Among various positioning techniques, the global position system (GPS) positioning, which decodes satellite signals to calculate the mobile device position, provide satisfying positioning results in the outdoors. However, since four or more satellite signals are required to be detected, indoor positioning with GPS can not locate the device due to the signal blocking by the buildings. On the other hand, wireless localization decides positions with the information of distances or angles extracted from the signals emitted from the wireless communications such as cellular [1], wifi [2], and bluetooth systems. Indoor positioning can be supported in these communication system with the firmware upgrade or software implementation.

For indoor positioning, to overcome the multipath condition especially in the non-line-of-sight (NLoS) condition when the direct path is blocked, fingerprinting based method is utilized by recording the signal characteristic at a certain environment at the offline stage. At the online stage, the collected measurements are compared with the offline database by finding the most similar measurement records. RSS-based fingerprinting [2], [3] has been studied for a long time and is regarded as a low-cost and high accuracy method in the indoor environment. K-nearest neighbor (KNN) [2] is one of the most representative RSS-based fingerprinting method.

Orthogonal frequency division multiplexing (OFDM) technology has become major physical layer technology in today's wireless communication such as wifi and 4G systems. To fully utilize the benefit of multi-carrier system under larger bandwidth, channel estimation is necessary to capture channel frequency response (CFR) on different subcarrier. The inverse Fourier transform of the CFR is the channel impulse response (CIR), which illustrates the paths the signal travelled from the position of the transmitter to the one of the receiver. Since CIR or CFR can be regarded as a signature for the position of receiver, the CIR-based location estimation method [4]–[6] can be utilized to enhance the accuracy of indoor location estimation. Note that the multipath effect deteriorates the quality of the results of the RSS-based measurement at smaller system bandwidth. However, with the expansion in the system bandwidth, the multipath effect diversifies signatures such as CIR. In general, the CIR-based method has better performance than the RSS-based method at larger system bandwidth when the time resolution is higher to distinguish the individual travelled paths.

To capture the effect of multipath, various research works [7]–[10] focus on how to measure and study the behaviors of multipath channels. The multipath model inside a certain building can only be generated based on the electromagnetic simulation, e.g., the ray-tracing (RT) method. The radiated waves are tracked via the penetration, reflection and diffraction to predict the channel response for a transmitter and a receiver pair. Moreover, the channel sounding systems are utilized to measure the preamble at the receiver to estimate the channel response. The challenges and methods are summarized for the channel measurement at 60GHz band in [9]. The power delay profile simulated using the sub-band ray-tracing method [10] has been validated to has high correlation with the channel measurement.

In this paper we focus on the fingerprinting based CIR method for indoor localization. To predict the channel characteristics, we utilize RT method [10], [11] to *simulate* the channel impulse responses with the same system bandwidth and the time resolution as the setting of the channel sounding. Moreover, we implement an OFDM-based channel sounding system to *measure* the channel impulse response. During the online stage, the measured channel frequency response sampled on each subcarrier is estimated using the channel sounding system. To differentiate the differences, the KNN concept to find K reference points with the highest correlation between the online measurement and the simulated CIR database is

[1]This work was in part funded by the the Technological University Paradigms, MOST 103-2221-E-027-030-MY2, MOST 103-2221-E-027-032-MY2, and the NTUT-BIT Collaborative Program.

978-1-4673-7211-4/15 $31.00 © 2015 IEEE
DOI 10.1109/UIC-ATC-ScalCom-CBDCom-IoP.2015.337

named as the RT-based fingerprinting (RBFP), which is a pure prediction method. The experiment is conducted to test the performance of the proposed RBFP.

II. System Architecture

The proposed RBFP algorithm can be implemented in the system architecture which includes the offline and online phases.

1) **Offline** stage: Two different sets of database is established for the positioning area in the offline stage. The OFDM-based channel sounding system includes the vector signal generator at the transmitter side and the vector spectrum analyzer at the receiver side. To collect signature of different positions, there are total N reference points (RPs) which measures from M transmitters *a.k.a.* access points (APs). To efficiently capture the statistic information, each RP forms a grid of S points separated by $a\ cm$ to cover an area of roughly $b\ m^2$. By placing the receiver at the ith RPs as two-dimensional (2-D) position (x_i, y_i), the receiver is capable of measuring the RSS $\hat{r}_j^M(i)$ and the CIR $\hat{\mathbf{h}}_j^M(i)$ from the jth transmitters (x_j, y_j). The measurement processes are repeated and the results are collected for the measurement database establishment. On the other hand, the same setting is applied for the ray-tracing technique to simulate the channel responses from all M APs to N RPs. The RSS $\hat{r}_j^R(i)$ and the CIR $\hat{\mathbf{h}}_j^R(i)$ from the ith AP to the jth RP are recorded as the simulation database.
2) **Online** stage: The channel sounding system is utilized to collect the online RSS measurements as a vector $\hat{\mathbf{r}}$ and the online CIR measurements as a matrix $\hat{\mathbf{h}}$. With the development of the OFDM-based channel sounding system, the conventional FP is perform by comparing the online measurement with the offline measured database. By utilizing the prediction of the RT technique, the proposed RBFP is utilized by comparing the online measurement with the offline simulation database. The 2-D position is estimated as $(\hat{x}, \hat{y})$.

III. Channel Impulse Response (CIR) Measurement

A. Ray-Tracing (RT) Simulation

RT simulation tool reflects the deterministic component of the channel between the transmitter and receiver given the simulation area. Instead of calculating electromagnetic radiation using numerous rays which is a computational complex task, ray tubes are calculated based on the triangular pyramids. The sphere of the transmitter and the surrounding environment are partitioned into triangular facets. The wave propagation including penetration, reflection, and diffraction is simulated using a triangular pyramid. A shooting and bouncing ray tracing method (SBR-RT) [12], [13] is implemented where the vector effective antenna height (VEH) concept is adopted when each ray encounter reflection. Note that scattering [10] is not considered in our RT software. In Fig. 1, the CIR, CFR, power delay profile (PDP), departure of angle (DOA), and arrival of angle (AOA) can be predicted given the environment of the transmitter and the receiver.

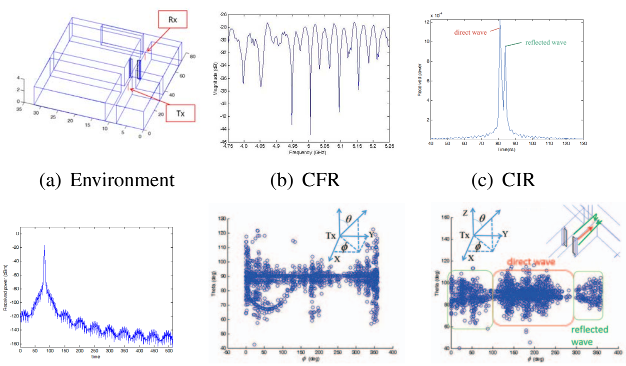

(a) Environment (b) CFR (c) CIR

(d) PDP (e) DOA (f) AOA

Fig. 1. Ray Tracing Simulation Result

RT simulator is implemented using the C++ object-oriented programming using Microsoft visual studio 2010. The flow of RT simulation is summarized as below.

1) *Environmental parameter settings*: An indoor 3-D map should be established and each sphere such as wall, ground, or obstacle is divided into triangular facets. The dielectric constant and the electric conductivity of the material associated to each facet in the indoor environment, e.g., concrete walls or glasses, should be recorded. The received electric field is also affected by the resolution of ray tubes as V, ray receiving rebound penetration times, transmission frequency and antenna patterns.
2) *Ray tubes generation*: Ray tubes are generated based on the above parameters and each ray tube is traced by calculating the normal vector of the emitting direction, which can determine if a certain sphere is reached.
3) *Receiver receiving the ray tube*: Providing that the receiver is inside the region contained by the ray tube (i.e., inside the triangular pyramid), the ray tube is received. The LOS path exists if the ray tube is not blocked, while the penetration through the wall should be considered for the calculation of electric field if the ray tube is blocked. The associated voltage induced by the ray is then calculated.
4) *Ray tube being blocked*: If the ray tube is not received by the receiver, it might be blocked by certain obstacle. The effective VEH should be calculated and a new ray tube is generated from the image position of the source for either the reflection or diffraction. Note that the bounce time of this ray tube is increased by one.
5) *Maximum bounce time being reached*: Providing that the maximum bounce time is reached, the contribution of this ray to the received electric field is marked as zero.
6) *End of RT simulation*: The program is ended if all the ray tubes are successfully received.

B. OFDM Channel Sounding System

The hardware acts as the RF front-end of the transmitter and the receiver of the sounding system, which supports up to 6GHz band and 100MHz bandwidth measurement. At the transmitter side, Agilent E4438C vector signal generator (VSG) is utilized for the signal generation at the desired band. The digital baseband sounding signal generated from the software is transferred to the analog signal and up-converts to the desired band by the VSG. A power amplifier is connected and the Hertzian dipole antenna is utilized for radiation. At the receiver side, Tektronix RSA 6114A vector spectrum analyzer (VSA) is utilized after the low-noise amplifier. The VSA down-converts the reception of RF signals to baseband and performs coarse timing estimation. The received signal is utilized for the channel estimation. Note that the hardware architecture has higher flexibility in system maintenance and algorithm development.

Quality of channel estimation depends on synchronization in both time and carrier frequency. Baseband algorithms for calibration and channel Estimation are required for the OFDM-based channel sounder. Imperfect time synchronization leads to inter-symbol interference (ISI) between OFDM symbols, while failure in frequency synchronization causes inter-carrier interference (ICI) between subcarriers. Both interference introduces bias in channel estimation. To overcome the ISI problem, two stages of time synchronization as coarse and fine timing synchronizations are considered. In order to ensure the existence of an OFDM symbol in the received signal, coarse timing synchronization is realized by received power level trigger with a built-in function in VSA. On the other hand, fine timing synchronization is to detect the exact starting index of an OFDM symbol. In [14], we have proposed a maximal power path detection method to realize fine timing synchronization with cross-correlation method. On the other hand, we assume that the carrier frequency offset is calibrated at RF front-end during the offline stage. Due to the flexibility in digital down-conversion and the superiority in RF device quality of the VSA, the frequency calibration is achieved by VSG sending carrier signal. The rate of change in the carrier phase is estimated and the VSA center frequency is corrected using the amount of estimated rate of change. The CFR can be estimated by the least squares (LS) estimation and the CIR is obtained by the inverse FFT.

IV. Proposed Ray-Tracing Based Fingerprinting Algorithm (RBFP)

The offline stage for the proposed RBFP is to create database by RT simulation using multi-carriers. To capture the statistical variation of the frequency response, the CIR of a RP is represented as the average of its associated S grids as $\hat{\mathbf{h}}_j^R(i)$. The variance of the CIR $\sigma^2_{\hat{\mathbf{h}}_j^R(i)} = Var[\hat{\mathbf{h}}_j^R(i)]$ is calculated for the weighting of fingerprinting. Note that RT-predicted RSS from the j-th AP to i-th RP can be obtained by summing L samples of CIR as $r_j^R(i) = \sum_{p=1}^{L} \hat{\mathbf{h}}_j^R(i)$. Therefore, RT-predicted RSS can be regarded as another statistical measure of channel impulse/frequency response but without the information of each sample/subcarrier. The RSS can be also utilized for positioning purpose.

During the online stage, the CFR from the j-th AP to the receiver can be estimated by the OFDM-based sounding system as $\hat{\mathbf{H}}_j$. Therefore, the measured CIR (i.e., $\hat{\mathbf{h}}_j$), the RSS (i.e., r_j) and the variance of CIR (i.e., $\sigma^2_{\hat{\mathbf{h}}_j}$) from the j-th AP to the receiver can be estimated as $\hat{\mathbf{h}}_j = F^{-1}\{\hat{\mathbf{H}}_j\}$, $r_j = \sum_{i=1}^{L} \hat{\mathbf{h}}_j$ and $\sigma^2_{\hat{\mathbf{h}}_j} = Var[\hat{\mathbf{h}}_j]$ accordingly.

A. CIR-based RBFP

Unlike traditional FP method, the proposed RBFP compares the online CIR measurement $\hat{\mathbf{h}}_j$ from the j-th AP with the RT-predicted database from the j-th AP to all the RPs to find out which RP has similar measure as the receiver. The correlation between the measured CIR from the j-th AP to the receiver as the online measurement and the predicted CIR from the j-th AP to the i-th RP as the offline measurement is adopted for the similarity measure

$$\rho_{\text{RBFP}_j}(i) = \rho_{\text{RBFP}_j}(\hat{\mathbf{h}}_j, \hat{\mathbf{h}}_j^R(i)) = \left| \frac{cov(\hat{\mathbf{h}}_j, \hat{\mathbf{h}}_j^R(i))}{\sigma_{\hat{\mathbf{h}}_j} \sigma_{\hat{\mathbf{h}}_j^R(i)}} \right| \tag{1}$$

Note that the subscript j of the RBFP in (1) represents the current signal is transmitted by the j-th AP. The larger value of $\rho_{\text{RBFP}_j}(i)$ represents that the position of the receiver is closer to the i-th RP. When receiving the signal from the j-th AP, the position of the receiver can be estimated by maximizing the cost function by defining the cost function $f_{\text{RBFP}_j}(i)$ to select the i-th RP of the proposed RBFP as $\rho_{\text{RBFP}_j}(i)$, i.e., $f_{\text{RBFP}_j}(i) = \rho_{\text{RBFP}_j}(i)$. The union of the set of indexes of RP with K-largest correlation between the online measurement and offline database is represented as $\mathcal{I}_{\text{RBFP}_j}$. For example, for the case $K = 3$, the set $\mathcal{I}_{\text{RBFP}_j}$ includes the three indexes of RPs where their offline prediction has the largest correlation with the online measurement from the j-th AP. Therefore, the position of user is estimated as average position of the RPs in the set $\mathcal{I}_{\text{RBFP}_j}$ as

$$\hat{\mathbf{x}}_{\text{RBFP}} = \sum_{i \in \mathcal{I}_{\text{RBFP}_j}} w_{j \to i} \cdot \mathbf{x}_i \ . \tag{2}$$

The weight $w_{j \to i}$ is defined for the j-th AP to the i-th RP and the RP with the K-largest correlation has a equal weight $w_{j \to i} = \frac{1}{K}$ in the design.

B. RSS-based RBFP

Besides the CIR measurement, the proposed RBFP can be also adapted to the RSS measurement. The cumulative distribution functions of position errors for the proposed schemes under two different transmitted antennas are compared in Figs. 4(b) and 4(c). Unlike multiple taps of CIR measurement can be obtained as a vector for the correlation calculation, the cost function of RSS is designed by using the difference between the online measurement of the average RSS in the database. The average RSS of the offline measurement is represented as $\mu_{r_j(i)} = avg[\hat{r}_j(i)]$. For example, the cost function for the

RSS of the proposed RBFP from the j-th AP can be calculated as

$$f_{\mathrm{RBFP}_j}(i) = \frac{1}{|\hat{r}_j - \mu^R_{r_j(i)}|} \tag{3}$$

Since the minimum difference between the online measurement and the offline data of the i-th RP represents the highest similarity of its signature between the current position and the i-th RP, the minimum RSS difference is utilized for RSS fingerprinting. However, to align with the CIR measurement which find the maximum cost, the reciprocal of the RSS distance is adopted as the cost function for the proposed scheme. The process of finding the maximum cost for the position estimation is then adopted for the RSS-based RBFP scheme.

V. Performance Evaluation

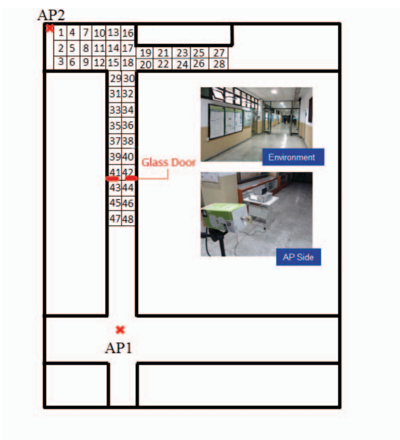

Fig. 2. Experimental Environment in Integrated Complex building 2F, National Taipei University of Technology

By implementing the OFDM-based sounding system in subsection III-B and the RT simulation program in subsection III-A, the proposed RBFP scheme is validated in the corridor of the second floor in the Integrated Complex Building of the National Taipei University of Technology, Taipei, Taiwan. Note that the material of the experimental environment is mainly composed of the concrete wall and the glasses window/door. The transmission frequency is within 850 MHz to 950 MHz while the transmission bandwidth is 100 MHz. The dielectric constant for concrete wall ϵ_r=6 while the electric conductivity for concrete is σ=0.01 s/m while that for the ceiling and ground are $\epsilon_r = 4$ and $\sigma = 0.02$ s/m. For the glass wall, ϵ_r is 3 and σ is 1×10^{-9} s/m. The polarizations of the transmitted and the received antennas are vertical. An icosahedron is constructed to describe a unit circle, where the facets of an icosahedron to is partitioned into for total $20 \times 50 \times 50$ ray tubes. The maximum number of bounce is 7 for tracing a ray tube and the ray is discarded when the bounce time reaches over the maximum. To obtain statistical measure such as power delay profile, a grid is further partitioned into 25 square regions. As shown in Fig. 2, The corridor of Complex building 2F, National Taipei University of Technology, with 45 m × 25 m × 3.5 m. The network is partitioned into 48 RPs, each with 1.7 x 1.7 m. Each RP is measured within 25 grids around and the spacing between two grids is 17 cm.

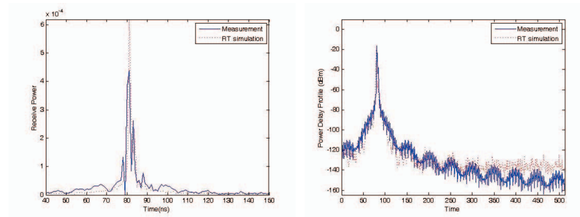

(a) Channel Impulse Response (b) Power Delay Profile

Fig. 3. Validation of Ray Tracing when the distance between transmitter and receiver is 8.5m.

In Fig. 3, the CIR/PDP predicted by the SBR-RT and the CIR/PDP measured by OFDM baseband sounding system are examined within a transmitter and a receiver where their distance is 8.5 m. PDP in terms of spatial diversity is calculated as

$$\hat{p}(\tau) = \frac{1}{S}\sum_{m=1}^{S}(\sum_{i=1}^{L}|\hat{\mathbf{h}}_j(t,\tau)|^2) \tag{4}$$

In general, the measured and predicted CIR/PDP measurements have power difference, which is ought into *(i)* the measurements are perturbed by the thermal noises and varied in different atmospheric temperature and humidity; *(ii)* the simulated environment for the RT is not modeled in details, e.g., the material factor of concrete wall is different if there are pit walls. These factors lead to the imperfection of the prediction. The similarity for the measured and predicted CIR/PDP can be observed in Fig. 3, which demonstrates the possibilities of utilizing the RT predicted data as the offline database.

One of the key parameters of the proposed RBFP is how the value of K should be chosen. The RPs with the K largest correlation are considered for the position estimation. To address this issue, we conducted an experiment in Fig. 4(a) to estimate the position using $K = 1$ to 5 for the experiment using the 67% position error of AP_1 and AP_2. Fig. 4(a) can be seen from the method with $K = 3$, allowing error distance to a minimum. Note that the position of the receiver is determined by K-nearest RPs. Since the position of the receiver has very low probability to be right on the RP, the receiver is usually confined by 3 or 4 RPs. There is insufficient amount of information if only K is chosen 1 or 2. However, if $K = 5$ is chosen, the correlation is decreased significantly for near neighbor RPs which has similar correlation as RP far away. Including larger neighbor causes worse performance by the misjudgment from the data and the computational complexity also increased. To achieve the tradeoff between performance and complexity, $K = 3$ is adopted in the following cases.

Since the CIR provides the signatures into each tap, the performance of utilizing the CIR measurement is better than

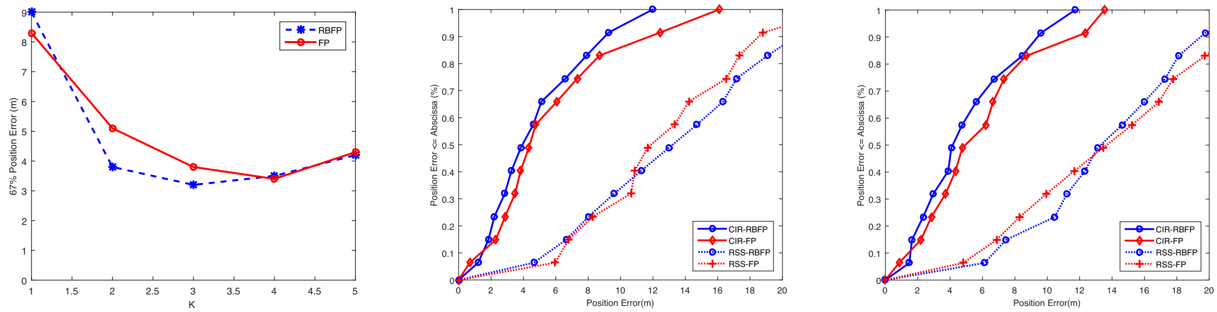

(a) 67% position error v.s. different K value

(b) Position Error using AP_1

(c) Position Error using AP_2

Fig. 4. Validation of the proposed RBFP scheme.

RSS. Note that the absolute value of the RSS measurement might not be accurately predicted by the RT-based method. Predicted database might not suitable for the RSS-based RBFP. However, the multipath signature can be provided by the RT, where the RBFP-CIR has compatible performance as the FP-CIR. The RT provides stable response such as the main reflection and diffraction from the surrounding environment and the concern is how accurate the RT can predict the response. Since the similarity of the predicted and measured data can be observed from Fig. 3, the result is convincible to use the RT simulation to replace the offline measurement collection. The offline measurement collected by the 25 grids and each with 50 times average might still contain temporarily noise and interference, which are random and differ from the online measurement.

VI. Conclusion

In the wireless OFDM broadband systems, the channel impulse response (CIR) measured for channel equalization and the received signal strength (RSS) measured to indicate the signal quality can be used as positioning signatures. OFDM-based channel sounding system and the ray-tracing (RT) method are implemented for the respective channel measurement and prediction. With the similarity between the measured and predicted channel, the RT-predicted data is further adopted to assist the localization. The conventional fingerprinting (FP) matches the online measured signatures with the offline ones to decide the receiver's position. The proposed ray-tracing based fingerprinting (RBFP) finds the position with the similarity evaluated with the online measured signatures and the RT-predicted data. The position prediction errors of both schemes are comparable because of the similarity of the offline measured CIRs and the RT-predicted data. Therefore, RT prediction can replace the role of offline channel measurement in conventional FP, reducing the cost of data collection and database build-up.

References

[1] K.-T. Lee, P.-H. Tseng, C.-H. Chen, and K.-T. Feng, "Femto-Assisted Location Estimation in Macro/Femto Heterogeneous Networks," in *IEEE Wireless Communication and Networking Conference (WCNC)*, Apr. 2013, pp. 1–5.

[2] H.-X. Liu, B.-A. Chen, P.-H. Tseng, K.-T. Feng, and T.-S. Wang, "Map-aware Indoor Area Estimation with Shortest Path Based on RSS Fingerprinting," in *IEEE Vehicular Technology Conference (VTC) Spring*, May 2015, pp. 1–5.

[3] C. Meng, Z. Ding, and S. Dasgupta, "A Semidefinite Programming Approach to Source Localization in Wireless Sensor Networks," *IEEE Signal Process. Lett.*, vol. 15, pp. 253–256, 2008.

[4] C. Nerguizian, C. Despins, and S. Affes, "Geolocation in mines with an impulse response fingerprinting technique and neural networks," *IEEE Trans. Wireless Commun.*, vol. 5, no. 3, pp. 603–611, Mar. 2006.

[5] Y. Jin, W.-S. Soh, and W.-C. Wong, "Indoor Localization with Channel Impulse Response based Fingerprint and Nonparametric Regression," *IEEE Trans. Wireless Commun.*, vol. 9, no. 3, pp. 1120–1127, Mar. 2010.

[6] K. Wu, J. Xiao, Y. Yi, D. Chen, X. Luo, and L. Ni, "CSI-Based Indoor Localization," *IEEE Trans. Parallel Distrib. Syst.*, vol. 24, no. 7, pp. 1300–1309, July 2013.

[7] J. He, K. Pahlavan, S. Li, and Q. Wang, "A Testbed for Evaluation of the Effects of Multipath on Performance of TOA-Based Indoor Geolocation," *IEEE Trans. Instrum. Meas.*, vol. 62, no. 8, pp. 2237–2247, Aug. 2013.

[8] N. Alsindi, X. Li, and K. Pahlavan, "Analysis of Time of Arrival Estimation Using Wideband Measurements of Indoor Radio Propagations," *IEEE Trans. Instrum. Meas.*, vol. 56, no. 5, pp. 1537–1545, Oct. 2007.

[9] W. Fu, J. Hu, and S. Zhang, "Frequency-Domain Measurement of 60 GHz Indoor Channels: A Measurement Setup, Literature Data, and Analysis," *IEEE Instrum. Meas. Mag.*, vol. 16, no. 2, pp. 34–40, Apr. 2013.

[10] P. Meissner, M. Gan, F. Mani, E. Leitinger, M. Frohle, C. Oestges, T. Zemen, and K. Witrisal, "On the use of ray tracing for performance prediction of uwb indoor localization systems," in *IEEE International Conference on Communications Workshops*, Jun. 2013, pp. 68–73.

[11] Z. Ji, B.-H. Li, H.-X. Wang, H.-Y. Chen, and T. Sarkar, "Efficient ray-tracing methods for propagation prediction for indoor wireless communications," *IEEE Antennas Propag. Mag.*, vol. 43, no. 2, pp. 41–49, Apr. 2001.

[12] S.-H. Chen and S.-K. Jeng, "SBR Image Approach for Radio Wave Propagation in Tunnels With and Without Traffic," *IEEE Trans. Veh. Technol.*, vol. 45, no. 3, pp. 570–578, 1996.

[13] ——, "An SBR/image Approach for Radio Wave Propagation in Indoor Environments with Metallic Furniture," *IEEE Trans. Antennas Propag.*, vol. 45, no. 1, pp. 98–106, 1997.

[14] Y.-C. Chan, P.-H. Tseng, D.-B. Lin, and H.-P. Lin, "Maximal Power Path Detection for OFDM Timing-Advanced Synchronization Schemes," in *IEEE International Symposium on Personal Indoor and Mobile Radio Communications (PIMRC)*, Sep. 2013, pp. 192–196.